Novel Polysilsesquioxane−I^-/I_3^- Ionic Electrolyte for Dye-Sensitized Photoelectrochemical Cells

Vasko Jovanovski,[†] Boris Orel,*[,†] Robi Ješe,[†] Angela Šurca Vuk,[†] Gregor Mali,[†] Samo B. Hočevar,[†] Jože Grdadolnik,[†] Elias Stathatos,[‡] and Panagiotis Lianos[‡]

National Institute of Chemistry, Hajdrihova 19, SI-1000 Ljubljana, Slovenia, and Engineering Science Department, University of Patras, 26500 Patras, Greece

Received: March 11, 2005; In Final Form: May 13, 2005

A new sol−gel precursor, based on 1-methyl-3-[3-(trimethoxy-λ^4-silyl)propyl]imidazolium iodide ($MTMSPI^+I^-$), was synthesized and investigated as a potential novel quasi-solid-state ionic liquid redox electrolyte for dye-sensitized photoelectrochemical (DSPEC) cells of the Graetzel type. $MTMSPI^+I^-$ was hydrolyzed with acidified water, and the reaction products of the sol−gel condensation reactions were assessed with the help of ^{29}Si NMR and infrared spectroscopic techniques. Results of time-dependent analyses showed the formation of a positively charged polyhedral cubelike silsesquioxane species, which still contained a small amount of silanol end groups that were removed after heating at 200 °C. After cooling, the material formed was a tough, yellowish, and transparent solid, consisting mainly of ladderlike polysilsesquioxane species. The specific conductivity (σ) of the nonhydrolyzed $MTMSPI^+I^-$ (no I_2) was 0.23 mS/cm, while the activation energy (E_a), determined from the Vogel−Tamman−Fulcher (VTF) relation, was 0.29 kJ/mol. After 56 days of aging the σ value of the hydrolyzed $MTMSPI^+I^-$ dropped to 0.11 mS/cm but the viscosity had already increased to 7500 Pa·s after 17 days, demonstrating that a quasi solid state was attained. Apparent diffusion coefficients (D_{app}) of I^- and I_3^- obtained from the voltammetric measurements were $\sim 10^{-7}$ cm^2/s and decreased to $\sim 10^{-8}$ cm^2/s after 15 days of sol aging. Time-dependent vibrational spectra, which served in assessing the hydrolysis and condensation reactions of $MTMSPI^+I^-$, were measured with the help of the attenuated total reflectance (ATR) IR spectroscopic technique. The results revealed that, in the course of condensation of sols, the refractive index of the modes attributed to the polysilsesquioxane species exhibited strong dispersion, which led to a shift of the vibrational band position in the experimental ATR spectra. This effect accompanies the sol-to-gel transformations and has not yet been considered as a possible error in analysis of the ATR spectra of sols and gels. The calculation procedure for obtaining the corresponding transmission spectra is briefly outlined, and the results are applied in this work.

Introduction

The first studies of dye-sensitized photoelectrochemical (DSPEC) cells date back to 1976, when Tsubomura[1] described a cell with a light-to-electricity conversion efficiency of less than 1%. After the discovery of O'Reagan and Graetzel[2] in 1990, that derivatives of ruthenium bipyridyl can effectively sensitize nanocrystalline TiO_2 for visible light absorption, the development of DSPEC cells commenced in various laboratories worldwide. An impressive 10% efficiency was already reported in 1995,[3] and further progress is anticipated due to the recently developed amphiphilic polypyridyl ruthenium dye, which has undoubtedly injected new momentum into this field.[4,5] DSPEC cells are currently considered as an auxiliary source of electricity, as substitutes for standard silicon photovoltaic cells. However, before their commercialization is possible, the sealing of volatile organic solvent-based electrolytes containing redox I^-/I_3^- couples and the long-term stability of these cells are issues that require resolution. With this in mind, p-type inorganic semiconductors,[6−9] organic hole-transport materials,[10−12] and polymeric materials incorporating I^-/I_3^- redox couples[5,13−16] have been considered as solid- or semi-solid-state substitutes for liquid DSPEC cells. Among these materials, sol−gel based redox electrolytes[17] have been extensively studied in our laboratory. They show semi-solid-state (i.e. gel-type) consistency because the reactive alkoxysilane groups terminating the long or medium-length poly(propylene glycol) chains cause the sols to condense into gels. The addition of sulfolane was found to beneficially affect cell efficiency, which can reach ~5%,[18,19] and simultaneously to increase their long-term stability. Sulfolane also prevents crystallization of KI, a problem encountered in DSPEC cells made solely with sol−gel based poly(propylene glycol) hybrids.[20] However, below 15 °C sulfolane solidifies, resulting in cracking of the electrolyte and a considerable drop in the cell performance. This prompted us to search for a nonvolatile yet liquid substitute for sulfolane.

Ionic liquids based on dialkylimidazolium cations with iodide[21] or other anions (BF_4^-, PF_6^-, etc.)[22,23] have been extensively considered as nonvolatile substitutes for liquid electrolytes in DSPEC cells. Since ionic liquids already act as a source of iodide and because the high viscosity of ionic liquids does not seem to affect their ionic conductivity, they represent a viable option for the fabrication of quasi-solid-state redox electrolytes. Solidification of ionic liquids was attempted through the addition of solid particles such as silica nanoparticles,[24] colloidal titania, and carbon nanotubes,[25] and by incorporation of ionic liquids in polymers.[26−28] The addition of small molecular weight

* Corresponding author. Telephone: 00386-1-4760-276. Fax: 00386-1-4760-300. E-mail: Boris.Orel@ki.si.
[†] National Institute of Chemistry.
[‡] University of Patras.

10.1021/jp051270c CCC: $30.25
Published on Web 07/08/2005

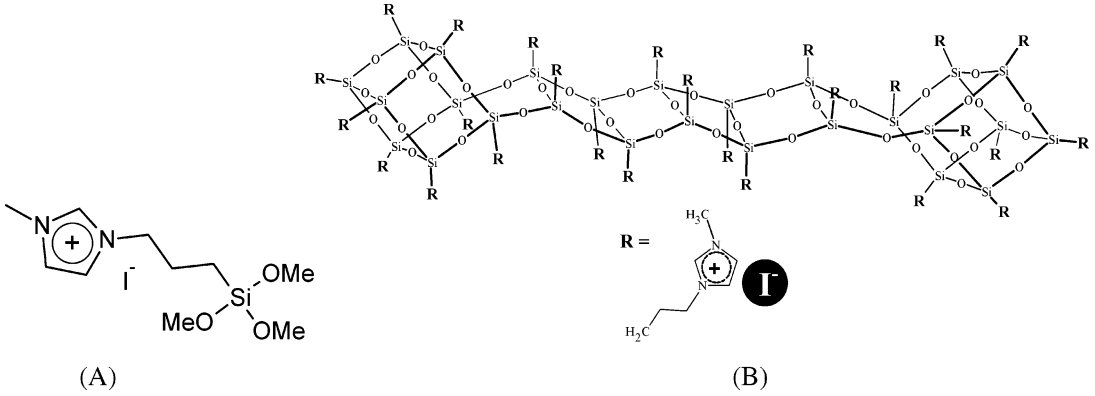

Figure 1. (A) Structure of 1-methyl-3-[3-(trimethoxy-λ^4-silyl)propyl]imidazolium iodide (MTMSPI$^+$I$^-$) ionic liquid and (B) probable structure of condensation species characterizing the quasi-solid-state ionic liquid.

gelators also seems to be effective,[29−32] and so does the addition of sol−gel tetramethoxysilane (TMOS) and *N*-[3-(triethoxy-λ^4-silyl)propyl]-1*H*-benzimidazole-1-carboxamide (ICS-BIM) precursors.[19] Their incorporation led to gelling of the 3-[2-(2-methoxyethoxy)ethyl]-1-methyl-1*H*-imidazolium iodide (MEOII) ionic liquid electrolyte, imparting an efficiency of up to 6% to DSPEC cells, the highest known thus far.[18,19] One of the most interesting variants is the preparation of polymeric solvent-free anionic conductors consisting of positively charged imidazolium polymeric chains and iodide[33] or polysiloxane with quaternary ammonium side groups.[34,35]

Recently, we synthesized a new imidazolium iodide type ionic liquid, namely MTMSPI$^+$I$^-$ (Figure 1A), which due to the trimethoxysilane groups, exhibits self-assembling properties, providing polymeric ionic liquid electrolytes, and imparting to the DSPEC cell a light-to-electricity efficiency of about 3.3%. Further study of the DSPEC efficiency is underway and will be published in a subsequent paper. In this study we aimed to elucidate the structure of the novel quasi-solid-state I^-/I_3^- ionic electrolyte for DSPEC cells and correlate these data with its specific conductivity, viscosity, and electrochemical properties.

The MTMSPI$^+$I$^-$ ionic liquid shown in Figure 1A is converted to a polymeric ionic liquid electrolyte after the execution of hydrolysis and condensation reactions. The trialkoxysilyl end groups of various alkyltrialkoxysilanes (R−Si(OR)$_3$), when hydrolyzed, enable polycondensation into crystalline or amorphous silsesquioxanes with complex (T cubelike or ladderlike) structures.[36,37] Most of the basic studies on the structure of polycondensation products of alkyltrialkoxysilanes have been carried out for simple alkoxysilanes such as hydrogen-, methyl-, phenyl-, or hexyl-substituted triethoxy- and trimethoxysilanes using ^{29}Si NMR,[37−40] X-ray diffraction,[41,42] rheological,[41,43] and infrared spectral measurements.

The assignment of the vibrational bands appearing in the IR spectra of oligosilsesquioxanes and the corresponding polyhedral condensation products obtained under acidic[44−48] and basic[49−51] catalysis conditions are surprisingly accurate, considering the fact that most of them were obtained nearly four decades ago. Their assignment was later confirmed by normal-coordinate analysis, which was performed mainly for hydrogen silsesquioxanes.[52−56] Fewer infrared spectroscopic studies were devoted to studying hydrolysis−condensation reactions of alkyl-substituted trialkoxysilanes leading to polysilsesquioxanes, which is surprising considering that both early[57] and more recent[58−60] spectroscopic studies done on hybrids consisting of TMOS, 3-(trimethoxysilyl)propyl methacrylate (TMSM) and methyl methacrylate (MMA) monomers,[58,59] and phenyltriethoxysilane[60] revealed that it is possible to make real-time measurements using IR spectroscopy. This method allows assessment of the loss of alkoxy groups, the formation of silanols, and the consequent establishment of siloxane linkages and characterization of condensation products (polyhedral silsesquioxanes, linear and cyclic species). Accordingly, in the present study the IR ATR (attenuated total reflection) spectroscopic technique was extensively used to follow the condensation of MTMSPI$^+$I$^-$ under acidic hydrolysis conditions. Such studies have not yet been performed, and no information exists as to whether T structures, ladderlike structures, or a mixture of these two types of condensation products forms under these hydrolysis conditions.

Initially, in situ time-dependent ATR spectra of sols aged to various extents were collected, which revealed that the ATR data did not satisfactorily reproduce the IR absorption spectra obtained in the transmission mode. This led us, in the subsequent step, to calculate the absorption spectra of sols in different stages of condensation from experimental ATR spectra. A previously reported calculation procedure[61−64] was used for this purpose. On the basis of the calculated absorption spectra, final assignment of the vibrational bands attributed to the aged MTMSPI$^+$I$^-$/HCl$_{aq}$ mixtures was obtained and correlated with the ^{29}Si NMR spectra of the hydrolyzed ionic liquid in various stages of aging.

Besides the formation of polyhedral silsesquioxane, the most interesting information obtained from these studies was the discovery that the formation of highly condensed species in MTMSPI$^+$I$^-$ (no I_2) sols hydrolyzed with acidified water was accompanied by a relatively small decrease of the specific conductivities and a slight increase in the activation energy determined from the Vogel−Tamman−Fulcher (VTF) relation. To substantiate the formation of the redox electrolyte, apparent diffusion coefficients (D_{app}'s) of I^- and I_3^- were determined from the steady-state voltammetric measurements of the hydrolyzed MTMSPI$^+$I$^-$ with and without added iodine. From the spectroscopic studies, and supported by viscosity measurements, the structure of the condensation species, constituting a quasi-solid-state redox electrolyte, was proposed as shown in Figure 1B.

Experimental Section

Materials. The synthesis of 1-methyl-3-[3-(trimethoxy-λ^4-silyl)propyl]imidazolium iodide (MTMSPI$^+$I$^-$) was as follows: 39 g (0.134 mol) of 3-iodopropyltrimethoxysilane (ABCR) was added to a solution of 11 g (0.134 mol) of 1-methylimidazole in 100 mL of 1,1,1-trichloroethane (Fluka). The mixture was then refluxed for 12 h and the ionic liquid decanted from the hot solution in a separatory funnel, washed

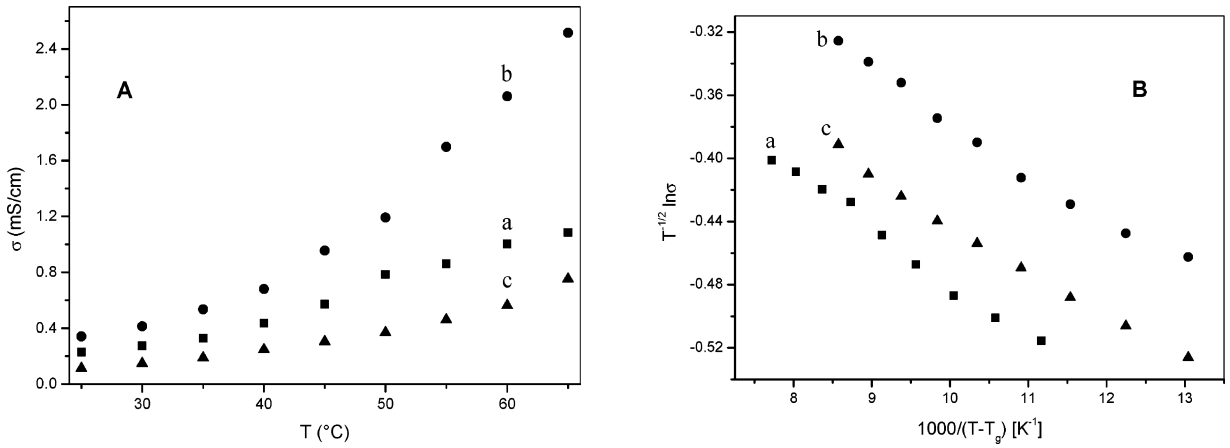

Figure 2. (A) Changes in specific conductivity with temperature and (B) Vogel−Tamman−Fulcher (VTF) plot: nonhydrolyzed $MTMSPI^+I^-$ (squares, curve a) and hydrolyzed $MTMSPI^+I^-$ aged for 24 h (circles, curve b) or 56 days (triangles, curve c).

twice with 100 mL of diethyl ether (Merck), and dried under reduced pressure. 1-Methyl-3-[3-(trimethoxy-λ^4-silyl)propyl]-imidazolium iodide (46.05 g) was obtained with a yield of 92%. The hydrolysis of $MTMSPI^+I^-$ was performed using 0.1 M HCl_{aq}.

Measurements. IR spectra were measured on a Perkin-Elmer System 2000 equipped with horizontal attenuated total reflectance (HATR, SpectraTech) and a Silver Gate ATR cell employing a Ge (refractive index $n = 4.00$) ATR prism. Sol−gel transitions have often been investigated with the help of ATR spectra measurements, primarily to follow spectral changes during the hydrolysis of precursors[63−65] and to assess the condensation products. The shifts of the siloxane bands and their intensity changes have been used to explain the formation of copolymers of tetraethoxysilane (TEOS) and diethyldiethoxysilane (DEDMS),[66] and cyclic and linear silica substructures in Nafion−silica composites,[67,68] using an ATR cell equipped with a KRS-5 ATR cystal ($n = 2.4$). Horizontal (HATR)[65−68] or circular ATR[65] attachments equipped with a ZnSe ATR crystal ($n = 2.4$) have been used in most cases, but Ge ($n = 4.0$) was sometimes applied as well. Unpolarized light was used for collecting the spectra, and the incidence angle was usually 45°.

When we used a ZnSe ATR crystal (incidence angle 45°) in our HATR attachment (SpectraTech), we noticed that the frequencies of the bands differed by up to 20 cm^{-1} with respect to those recorded with the same HATR attachment equipped with a Ge ATR crystal. Frequencies recorded with the Ge ATR crystal were always higher and matched better with spectra measured in the transmission mode. It seemed initially that, when a Ge ATR crystal was used, ATR spectra, which reproduced the corresponding transmission spectra of the gels to the greatest degree, could be obtained. However, the moderately intense band of MeOH measured in the HATR or Silver Gate cell was red-shifted by about 10−12 cm^{-1} from the frequency of this band in the transmission spectra (1033 cm^{-1}). Larger red-frequency shifts (up to 30 cm^{-1}) were noted for the much more intense siloxane modes (1200−1000 cm^{-1}). This means that the ATR spectra of the ionic liquids characterized by much stronger siloxane modes—even when a Ge ATR crystal was used—did not accurately reproduce the vibrational spectra obtained in the transmission mode. Accordingly, the method of quantitative analysis of ATR spectra developed by Bertie et al.[61] was used to obtain the IR absorption spectra of the ionic liquid samples. The optical constants (refractive index n and absorption coefficient k) were calculated, and the absorption spectra (A) were expressed by $A = 2\pi k\tilde{\nu}d_{ef}$ ($\tilde{\nu}$, wavenumber in cm^{-1}; d_{ef}, normalized thickness of the absorbing film (1 μm)). Transmission IR spectra of an as-prepared, i.e., not yet hydrolyzed, ionic liquid were obtained either by spreading it on a silicon wafer (thickness 0.3 mm) or by sandwiching it between two silicon wafers.

^{29}Si NMR spectra were recorded on a Varian Unity Plus 300 MHz spectrometer using a Doty CPMAS probe head. The Larmor frequency of the silicon nuclei was 60.190 MHz. Samples were spun about the magic angle with a frequency of 2 kHz. ^{29}Si chemical shifts were determined using DSS (sodium 3-(trimethylsilyl)propane-1-sulfonate) as an external standard and then expressed relative to TMS (tetramethylsilane) ($d = 0$ ppm).

Specific conductivity (σ) measurements were carried out in an electrochemical cell using platinum electrodes (the cell constant was determined with 0.1 M KCl) by ac impedance measurements (SOLARTRON 1250 frequency response analyzer and a SOLARTRON 1286 electrochemical interface) in the frequency range 0.1−65000 Hz. Cyclic voltammetry measurements were performed using a modular electrochemical workstation (Autolab, Eco Chemie) equipped with PGSTAT12 and ECD modules. The working electrode consisted of a platinum disk microelectrode ($a = 25$ μm), with an Ag/AgI electrode and a platinum wire acting as the reference and counter electrodes, respectively.

The rheological properties of the sample were determined using a rotational controlled stress rheometer (HAAKE RheoStress RS150), equipped with a plate-and-plate sensor system (HPP 25/0.5 mm gap). The hydrolyzed $MTMSPI^+I^-$ was kept in an open vessel at ambient conditions over the course of measurements (17 days) to condense, and a small part of the sample was taken from the batch and used to perform the viscosity measurements.

Results and Discussion

Electrical and Viscosity Measurements. Nonhydrolyzed $MTMSPI^+I^-$ and $MTMSPI^+I^- + I_2$: Fresh Samples. As shown in Figure 2A (curve a), the specific conductivity of the nonhydrolyzed $MTMSPI^+I^-$ is on the same order of magnitude as that for other 1,3-dialkylimidazolium iodide based ionic liquids,[21,69] but is approximately 10 times lower than that of ionic liquids containing other anions.[22,23] Upon increasing the temperature to only 60 °C, the specific conductivity increased from 0.23 to 1.00 mS/cm, reaching values similar to those of molten Bu_4NI[70] (i.e., 4.5×10^{-3} S/cm), which also does not contain triiodide ions.

The conductivity data were fitted to the Vogel−Tamman−Fulcher (VTF) relation, and an E_a value of about 0.29 kJ/mol

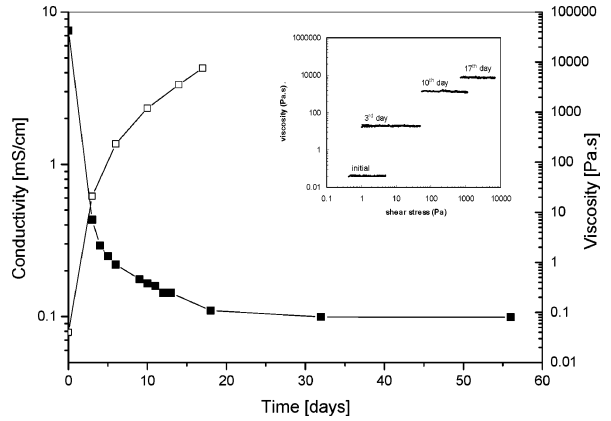

Figure 3. Changes in specific conductivity (filled squares) and viscosity (open squares) of hydrolyzed $MTMSPI^+I^-$ with aging. Inset: Newtonian behavior of hydrolyzed $MTMSPI^+I^-$ sol.

was determined taking into account a glass transition (T_g) value of −64.4 °C (Figure 2B, curve a). Similarly to the specific conductivity, the viscosity (η) of the nonhydrolyzed $MTMSPI^+I^-$ (η = 2.9 Pa·s) also agreed very well with the values of other ionic liquids[22,23,31,69] (see below).

By analogy with other ionic liquids and molten salts, the σ values of the nonhydrolyzed $MTMSPI^+I^-$ increased from 0.23 to 0.62 mS/cm when the iodine was added in concentrations from 0 to 0.74 M. The increase of the σ values could be easily explained for the nonhydrolyzed samples as being due to the formation of I_3^- or possibly polyiodide ions. Supporting evidence for the presence of I_3^- ions was obtained from Raman and UV−vis spectra (not shown here).

Hydrolyzed $MTMSPI^+I^-$ and $MTMSPI^+I^- + I_2$: Effect of Condensation. (a) Conductivity and Viscosity Measurements. Hydrolyzed $MTMSPI^+I^-$ that was aged for 24 h exhibited a similar temperature dependence on conductivity and slightly higher T_g and E_a values than the nonhydrolyzed sample (Figure 2A). As expected, the conductivities of the hydrolyzed samples were found to be dependent on aging (Figure 3) because of the execution of condensation reactions. During the first 3 days of aging, σ dropped severely to ∼0.4 mS/cm, but at longer aging times the decrease became less rapid, and after 20 days σ values stabilized at ∼0.1 mS/cm. A similar time dependence of specific conductivities with time of aging was also found for samples containing iodine. The most plausible explanation for the fast drop in σ values noted during the first days was the formation of a sol−gel matrix and release of MeOH and water due to condensation reactions (see below).

The most convincing evidence for the transformation of the hydrolyzed $MTMSPI^+I^-$ to a quasi solid state was obtained from measurements of the sample viscosity during aging (Figure 3). Measurements were performed under steady shear conditions (flow curves) at constant temperature (20 °C). The results revealed that, throughout the measurements, the viscosity was independent of the shear stress (Figure 3, inset). This means that the $MTMSPI^+I^-/HCl_{aq}$ sols remained Newtonian liquids, despite the fact that the viscosities steadily increased during the measurements. This result suggested that the type of interactions remained the same regardless of the size of the condensation products. The initial viscosity was 0.04 Pa·s, i.e., considerably smaller compared to the viscosity of the nonhydrolyzed samples (2.9 Pa·s), but it increased to 7500 Pa·s after 17 days. The small initial viscosity was attributed—by analogy with σ values—to the formation of MeOH and the addition of an acidified water catalyst. It is important to note that the specific conductivity of the ionic liquid in a quasi-solid-state consistency, determined after 56 days of aging, stabilized at 0.11 mS/cm (Figure 3), i.e., at a value only twice as small as that of the nonhydrolyzed $MTMSPI^+I^-$ (i.e., 0.23 mS/cm). Interestingly, the corresponding T_g and E_a values (Figure 2B) increased to −49.6 °C and 0.23 kJ/mol, most probably due to the establishment of additional conduction paths in the fully condensed sample. Molecular masses of the condensation products were not determined, as their precise determination requires the viscosity measurements to be accompanied by multiple light scattering measurements, which were not available in the laboratory.

Hydrolyzed $MTMSPI^+I^-$ and $MTMSPI^+I^- + I_2$: Effect of Condensation. (b) Steady-State Voltammetric Measurements. Apparent diffusion coefficients (D_{app}'s) are used to establish various correlations, which characterize either the DSPEC cell's properties (such as short-circuit current[15]) or the composition of the redox electrolyte. For example, D_{app} reflects the amount of the polymeric phase[5,27] or silica reinforcing particles[24] used to solidify the ionic liquid or cosolvent type redox electrolyte.[4] The ionic liquids synthesized by Bohnote et al.[21] and Matsui et al.[23] exhibited D_{app} values of about 10^{-7} cm^2/s, with these values remaining relatively unchanged when the ionic liquids were incorporated into organic polymers,[5,27] suggesting that during the solidifying process conduction paths for ions were established, thus enabling relatively unobstructed motion of I^- and I_3^-. For sol−gel glasses made from tetraethoxysilanes (TEOS) or tetramethoxysilanes (TMOS), studied extensively by Collinson et al.[71] and later by Niedziolka and Opallo,[72] D_{app} values dropped by 3−5 times when the sols gelled, even in the presence of cosolvents (sulfolane or propylene carbonate). This was attributed to the more restricted motion of ions in these types of silicate networks, which become more dense and where the average diameter of the pores decreases.[73] Because of the presence of a conducting cosolvent phase, the corresponding D_{app} values for ferrocene and Co(II)tris(bipyridine) redox reactants are on the order of 10^{-6} cm^2/s.

For the determination of D_{app} values, at least for quasi-solid-state ionic liquid electrolytes, the steady-state voltammetric measurements derived by Denault et al.[74] were applied in combination with ultramicroelectrodes. In the first step, the gelling of the hydrolyzed $MTMSPI^+I^-$ and $MTMSPI^+I^- + I_2$ was followed with cyclic voltammetric measurements (10 mV/s), as shown in Figure 4, to obtain information about the condensation reactions.

As expected, the anodic and cathodic peaks shifted over the course of aging, resembling the behavior of sol−gel glasses studied by Opallo et al.[72,73] For $MTMSPI^+I^-$ and $MTMSPI^+I^- + I_2$ the currents were not the same, indicating the formation of I_3^- (anodic scan) and I^- (cathodic scan), and decreased with time of gelling.

The apparent diffusion coefficient (D_{app}) values were determined from steady-state voltammetric measurements (Figure 5) using the equation $I = 4ncaFD_{app}$.[74] The results revealed that fresh hydrolyzed $MTMSPI^+I^-$ and $MTMSPI^+I^- + I_2$ exhibited almost the same $D_{app}(I^-)$ values of 2.1×10^{-7} cm^2/s (no I_2) and 1.9×10^{-7} cm^2/s (0.5 M I_2), while the D_{app} value of the I_3^- ions determined for the $MTMSPI^+I^- + I_2$ sample was 4.8×10^{-7} cm^2/s. All the values corresponded quite well with $D_{app}(I^-)$[24,27] and $D_{app}(I_3^-)$ values[4,15,27] determined for other systems with incorporated ionic liquids, but were about 10 times lower with respect to values determined from the time-course decay measurements of the radioactivity.[31] However, $D_{app}(I_3^-)$ of $MTMSPI^+I^- + I_2$ decreased over the course of aging to 5.1×10^{-8} cm^2/s (8th day) and 5.2×10^{-8} cm^2/s (15th day). Due

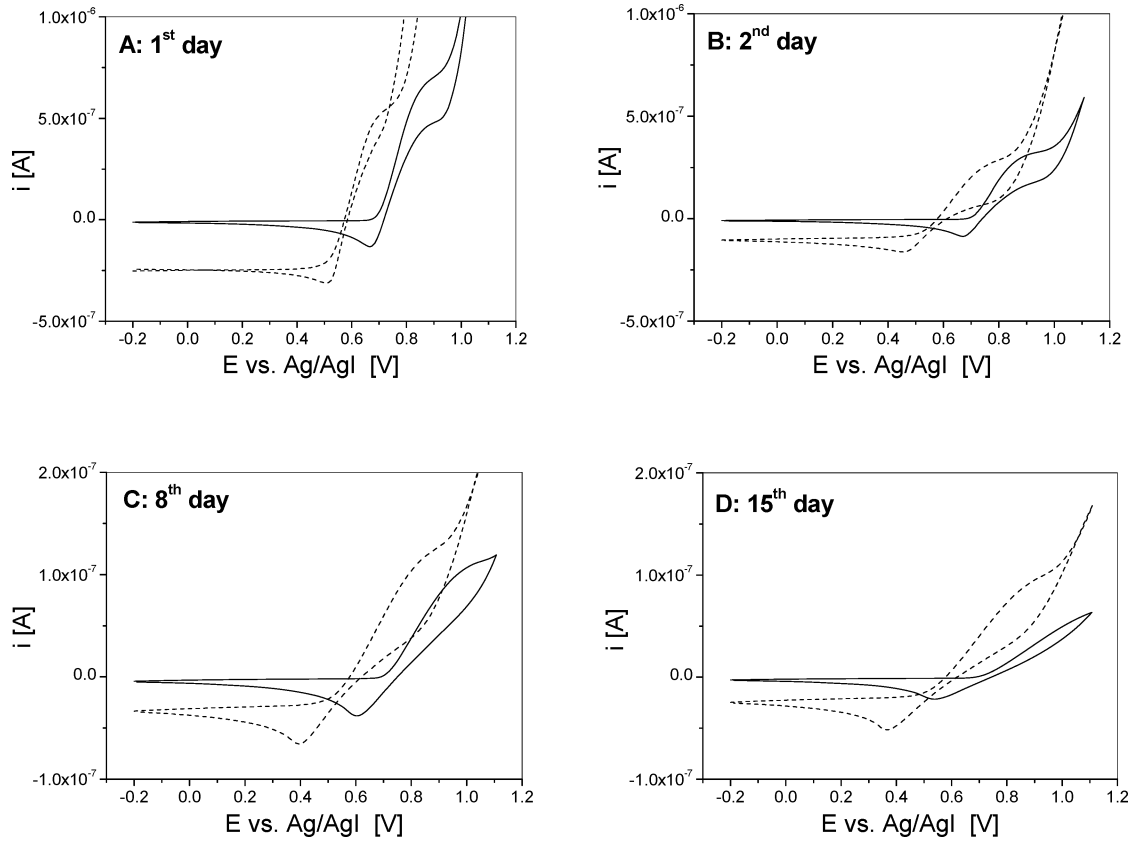

Figure 4. Cyclic voltammetric measurements (10 mV/s) of hydrolyzed $MTMSPI^+I^-$ (solid lines) and hydrolyzed $MTMSPI^+I^- + I_2$ (0.5 M) (dashed lines) during aging: (A) 1st, (B) 2nd, (C) 8th, and (D) 15th day.

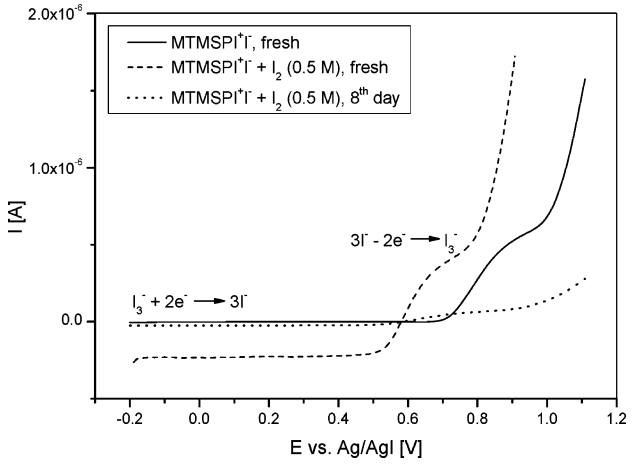

Figure 5. Steady-state voltammetric measurements (1 mV/s) of hydrolyzed $MTMSPI^+I^-$ and $MTMSPI^+I^- + I_2$ (0.5 M).

to condensation, cathodic limiting currents, for example, decreased from -2.3×10^{-7} A (fresh) to -2.5×10^{-8} A (8th day) for $MTMSPI^+I^- + I_2$, which might be attributed to a cessation in the mobility of the I_3^- ions due to the increased viscosity.

Structural Studies: Condensation to a Quasi Solid State. ^{29}Si MAS NMR Spectra. To obtain aditional information about the condensation products, ^{29}Si MAS NMR spectra of nonhydrolyzed and hydrolyzed $MTMSPI^+I^-$ were measured (Figure 6). The range of ^{29}Si chemical shifts of trifunctional alkoxysilanes ($R'Si(OR)_3$) extends from −35 to about −70 ppm[37] and is manifested by four groups of lines denoted by $T^n(i,j)$, where n represents the number of siloxane bonds attached to the silicon atom, and i and j indicate the number of −OH and −OR groups, respectively. Generally, in the course of aging, ^{29}Si NMR spectra of trialkoxysilanes show a shift of T^1, T^2, and T^3 signals to consecutively higher fields by the expected −8 ppm, indicating different condensation products. The exact assignment of T^2 and T^3 signals is a complex task, and as shown by Brunet,[40] the pattern of resonances from the hydrolyzed products is not characterizable by the predicted 2 ppm shift downfield, except for T^1. The signals in the T^1 region give a relatively clear picture of the single condensation reaction leading to dimers characterized by a single siloxane and zero, one, or two remaining −OMe groups. However, linear trimers and tetramers containing different numbers of remaining −OMe groups contribute to the T^1 and T^2 signals. In addition to this, cyclic trimers (T^2_{3C}) also resonate in the T^1 region (−47.85 ppm) but the signals of cyclic tetramers (T^2_{4C}) are less shifted from the usual T^2 region and appear at about−56 to −57 ppm.[40] Cagelike species are the main contributors to the signals in the region from −65 to −85 ppm, depending on the organic groups. Despite the complex situation, on considering the relative integrated intensity of the signals (Table 1, Figure 6) and taking into account the results of the infrared spectral analysis, some information about the type of condensation products of hydrolyzed $MTMSPI^+I^-$ was nevertheless obtained.

As revealed in Figure 6a, the nonhydrolyzed $MTMSPI^+I^-$ is characterized by a single $T^0(0,3)$ signal at −41.6 ppm, which correlates quite well the $T^0(0,3)$ signal of *n*-propyltrimethoxysilane at −42.8 ppm.[75] The additional weak signal at −49.9 ppm could be attributed to T^1 of the nonhydrolyzed dimers obtained during preparation of the sample. It is unlikely that these dimers formed during manipulation of the samples in air due to uncontrolled hydrolysis. In such a case, apart from the observed $T^0(0,3)$ signal, other signals attributable to the partially hydrolyzed species would be seen in the spectra ($T^0(1,2)$, $T^0(2,1)$, and $T^0(3,0)$) at more positive fields.[38]

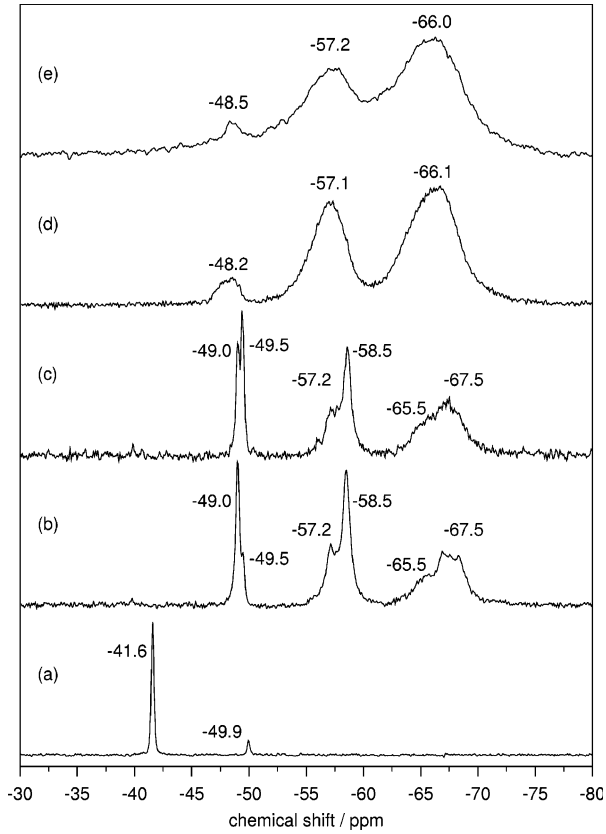

Figure 6. ^{29}Si NMR spectra of (a) nonhydrolyzed and (b−e) hydrolyzed MTMSPI$^+$I$^-$ in various stages of aging: (b) 2−3 h (initial), (c) 1 day, (d) 1 week, and (e) 2 weeks.

TABLE 1: Relative Integrated Intensity of T^1, T^2, and T^3 Signals Observed in ^{29}Si NMR Spectra of Hydrolyzed MTMSPI$^+$I$^-$ Samples in the Course of Aging

hydrolyzed MTMSPI$^+$I$^-$	T^1 [%]	T^2 [%]	T^3 [%]
2-3 h (initial)	18.0	42.5	39.5
1 day	20.5	36.0	43.5
1 week	6.0	37.0	57.0
2 weeks	2.0	33.5	63.3

During the few hours required for measurement of spectra of the hydrolyzed sample (Figure 6b), the $T^0(0,3)$ and T^1 signals at −41.6 and −49.9 ppm disappeared completely, suggesting the total loss of monomers[40] and the formation of partly hydrolyzed dimers and/or linear trimers. After 1 day (Figure 6c) the corresponding two T^1 signals (49.0 and 49.5 ppm) appeared with exchanged intensities, signaling that the number of dimers with more −OH groups had decreased, as these dimers were consumed to form cyclic tetramers, probably resonating at −57.2 ppm, and cubelike T^3 species (60−70 ppm). The consumption of dimers may also have been compensated by the formation of linear trimeric species that resonated in the T^1 region.[40] This was suggested by the increase in the relative integrated intensity of the T^1 signal of about 2.5% (Table 1) and from the small downfield shift of the signal at −48.99 ppm, which deviated from the 2 ppm downfield shift expected for −OH groups.

After 1 day of aging, the T^2 signal (Figure 6b,c, Table 1) decreased in relative integrated intensity by more than 6% due to a decrease in cyclic tetramers and the formation of cubelike species, which was characterized by an increase in T^3 signals at −65.5 and −67.5 ppm of 4%. It is important to note that cyclic tetramers were already formed in the initial stage of condensation (Figure 6b), as independently deduced from the band at 1100 cm^{-1} observed in the IR spectra (see section Infrared Spectra). A continuous blue frequency shift of the band at 1100 cm^{-1} and the growth of absorption in this region showed that after 1 day (Figure 6c) cyclic tetramers were partially consumed due to interaction with dimers and linear trimers. As a result of these interactions, larger cubelike species were formed, as shown by the characteristic T^3 signal in Figure 6c. The formation of cubelike species with three siloxane bonds already during the first day of aging seemed to be a characteristic feature of the condensation reaction of the hydrolyzed MTMSPI$^+$I$^-$ samples.

^{29}Si NMR spectra of the samples aged 2 weeks (Figure 6e) were characterized by broad downfield shifted signals at −48.5, −57.2, and −66.0 ppm. Broadening of the signals suggested the presence of various condensation species. The most obvious feature was the drop in the relative integrated intensity of the T^1 signal, which reached only 2%, and was not accompanied by a similar change of the T^2 signal (33.5% in Table 1). This fact indicated (when IR spectra analysis was taken into consideration) the presence of a relatively high number of bridging cyclic siloxanes but a small number of linear or cyclic trimers. The decrease in the T^1 signals could be unambiguously explained by, first, their condensation to cyclic tetramers (T^2) followed by condensation to open cubelike polyhedral species containing one or more silanol groups ($T_4(OH)_4$,[45,46] $T_7(OH)_3$,[46] $T_8(OH)_4$,[45] etc.). After prolonged aging (2 weeks, Figure 6e) the latter led to cubelike species as inferred from the T^3 signal (T_8, T_{10}, etc.). Analysis of the NMR spectra suggested a condensation process involving the formation of linear, cyclic, polycyclic, and, finally, polyhedral siloxanes. This idea, first expressed by Sprung and Guenther,[44] was further developed by Brown and Vogt[46] and Voronkov and Lavrentyev.[36]

The overall effect of the condensation reactions was a pronounced increase in cubelike species, the relative integrated intensity of which grew by 63% after 2 weeks (Table 1). In this respect, our system resembled other organically substituted trialkoxysilanes,[59,75,76] which do not gel under similar conditions. Although the NMR data did not give detailed information about the products formed in the course of aging, the strong T^2 signal (33.5% in Table 1) unambiguously confirmed the existence of polyhedral ($T_7(OH)_3$, $T_8(OH)_4$) species containing silanol groups, which enabled bridging to cubelike species. To obtain additional evidence about the possible beads-on-string or ladderlike structure of the aged sols, we performed IR spectroscopic analysis of the sols in various stages of aging.

Infrared Spectra. The vibrational bands collected from the IR transmission spectra of various condensation products from the acid hydrolysis of different oligo- and polysilsesquioxanes (cubelike and ladder type), together with the bands of cyclic and open-chain siloxanes, have already been reported in our previous publication.[64] The corresponding data provided the basis for the assessment of the condensation products formed in the course of aging of hydrolyzed MTMSPI$^+$I$^-$ sols.

Before extracting information about the nature of the species characterizing the process of condensation of hydrolyzed MTMSPI$^+$I$^-$ sols from the IR spectra, the most prominent bands of MTMSPI$^+$I$^-$ were identified by comparing its spectra with the spectra of other compounds containing similar groups, i.e., methyltrimethoxysilane, isopropyltrimethoxysilane, imidazol and 1-methyl-3-propylimidazolium iodide ionic liquid. The IR spectrum of nonhydrolyzed MTMSPI$^+$I$^-$ is relatively simple, exhibiting the dominant modes of −OMe groups (2844, 1194, 1080, 820, 775 cm^{-1}) in agreement with the corresponding bands of methyltrimethoxysilane (MTMS),[77] and also in concur-

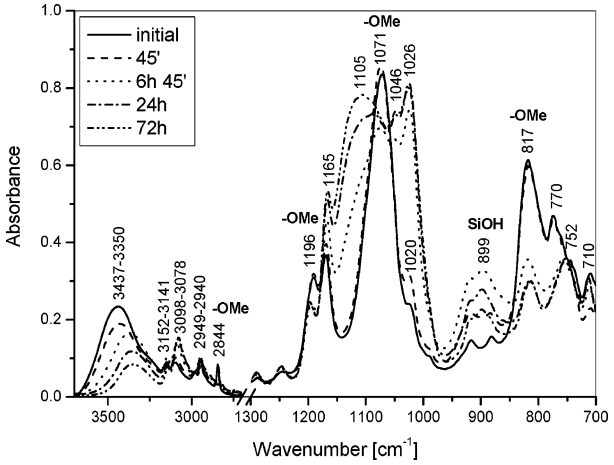

Figure 7. ATR spectra of hydrolyzed $MTMSPI^+I^-$ measured in the course of aging.

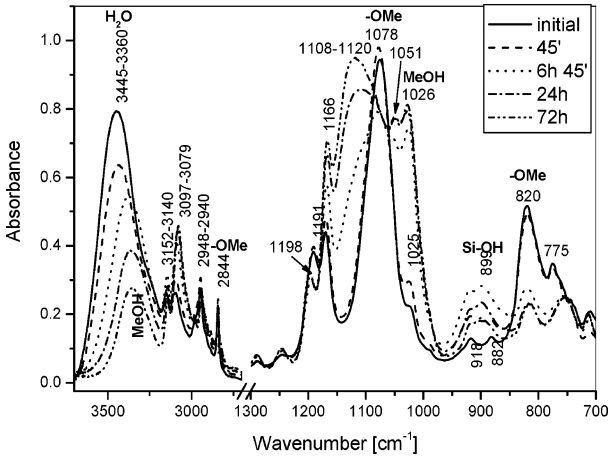

Figure 8. IR absorption spectra obtained from calculations of experimental ATR spectra depicted in Figure 7. Intensities were normalized to the sample thickness of 1 μm.

rence with the −OMe bands of tetramethoxysilane (TMOS).[78] Among the imidazolium modes, the ring modes at 1575 and 1170 cm^{-1} were strong enough to become apparent in the spectrum of the 1-methyl-3-propylimidazolium iodide ionic liquid,[69] also synthesized in our laboratory, and some other 1,3-dialkylimidazolium cation ionic liquids.[79] The C−H stretching mode of the imidazolium cation was assigned to the bands at 3140 and 3078 cm^{-1}, while the aliphatic C−H stretching modes appeared at 2976 and 2945 cm^{-1}.[80] The −OMe band at 2840 cm^{-1} did not interfere with other bands in the 3100−2800 cm^{-1} region, which represent a relatively pure group frequency attributed to $-CH_3$ stretchings of Si−OMe groups.[78] Hence this band, with other Si−OMe bands, was used to assess the degree of hydrolysis of $MTMSPI^+I^-$.

To establish the appearance of various products of the condensation reaction, the ATR method (Figures 7 and 8) was applied and the time variation of the intensity of siloxane (1000−1200 cm^{-1}), silanol (910−900 cm^{-1}), water (3300−3500 cm^{-1}), MeOH (1029−1033 cm^{-1}), and −OMe bands was assessed (Figure 9). Instead of using experimental ATR spectra directly (Figure 7), the corresponding absorption spectra were calculated[61−64] (Figure 8). Comparison of the band intensities and their frequencies in Figures 7 and 8 revealed that they were not the same; stronger bands appeared in the experimental ATR spectra of more condensed sols at lower frequencies and were less intense. These effects stemmed from the fact that ATR spectra are sensitive to variations in the refractive index (n) of

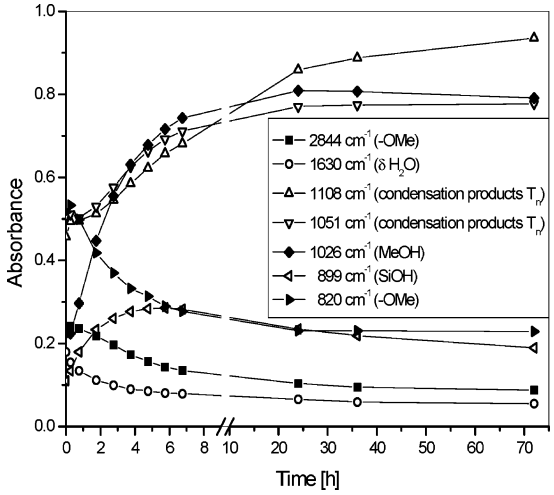

Figure 9. Intensity changes of IR bands vs time of aging.

the sample, which changed over the course of condensation. For example, the refractive index for the strongest siloxane band, for the aged and denser samples, varied in the region 1180−950 cm^{-1} from ∼2.39 to 2.62 ($\Delta n = 0.32$), while the initially hydrolyzed $MTMSPI^+I^-$ gave a value of between 2.44 and 2.57 ($\Delta n = 0.12$). To conclude, direct use of experimental ATR spectra inevitably leads to misinterpretations of the spectra and incorrect identification of the nature of the condensation products.

Figure 9 shows the variations in the intensity of the bands obtained from the calculated absorption spectra over the course of aging. The condensation process could be divided into two stages: the first appeared after 7−10 h and was characterized by strong changes in the intensities of nearly all the bands, while in the second stage only the Si−OH (∼900 cm^{-1}) and the siloxane bands in the 1000−1200 cm^{-1} region changed.

During the first stage of aging hydrolysis and condensation reactions took place simultaneously: the growth of the MeOH band (1026 cm^{-1}) was accompanied by a decrease in the intensity of the Si−OMe bands (2844, 1078, 820, 775 cm^{-1}) and a concurrent enhancement of the silanol band (∼900 cm^{-1}). Some other bands developed at 1022 cm^{-1} (cyclotrisiloxane),[77] 1051 cm^{-1} (open-chain three- or four-member siloxanes),[81,82] and 1090−1100 cm^{-1}. The latter band was attributable to one of the possible open cubelike condensation products such as $T_4(OH)_4$,[45,46] $T_7(OH)_3$,[46] and $T_8(OH)_4$.[45] The evidence for the presence of open cubelike species ($T_7(OH)_3$ and $T_8(OH)_4$) corroborated the observation of the T^3 signal in the ^{29}Si NMR spectra (Figure 6). An additional mode, contributing to absorption in the 1090−1110 cm^{-1} region, is the band of cyclic tetramers ($T_4(OH)_4$[45,46]) inferred from the T^2 NMR signals.

The second stage of aging (Figures 8 and 9) was characterized by condensation, as inferred from the slow decrease of the silanol band at ∼900 cm^{-1} and the concurrent growth of absorption around 1110 cm^{-1}. The final spectrum (72 h) showed a band at 1120 cm^{-1}, suggesting the presence of T_8 cubes.[36,46] This band was broad and extended to the 1100−1060 cm^{-1} region, signaling the coexistence of open cubelike silsesquioxanes such as $T_7(OH)_3$ (1112, 1086, 1068 cm^{-1}), $T_8(OH)_4$ (1109, 1060, 1045 cm^{-1}), or $T_6(OH)_2$ (1108, 1089, 1060 cm^{-1}), and was substantiated by the T^3 signal observed in ^{29}Si NMR spectra of aged (1 and 2 weeks) samples (Figure 6). Surprisingly, the band at 1051 cm^{-1}, attributed to open three- or four-member siloxanes, was still present in the spectra despite the fact that its intensity was expected to decrease due to the formation of open cubelike[81,82] species, which do not show absorption in this

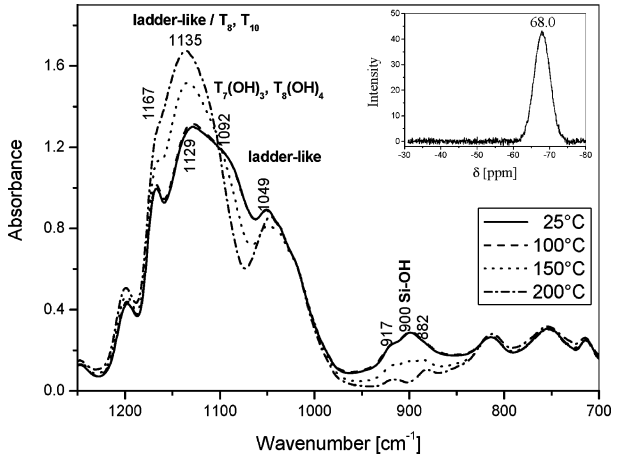

Figure 10. IR absorbance spectra of hydrolyzed $MTMSPI^+I^-$ aged 4 months and then heat-treated at various temperatures. Inset: ^{29}Si NMR spectrum of heat-treated (200 °C) sample.

region. To clarify this question, the samples were spread on silicon wafers and heat-treated at different temperatures, and the spectra were recorded in the transmission mode (Figure 10).

Inspection of the spectra recorded at room temperature revealed the absence of the MeOH band and the presence of well-developed bands at 1129 cm^{-1} (cubelike), 1092 cm^{-1} (open cubelike), and 1049 cm^{-1} (open three- or four-member siloxanes) (Figure 10). The silanol band at ~900 cm^{-1} was also noted, indicating that complete condensation was not yet attained. However, this band disappeared in the spectra of samples heated at 150 and 200 °C. As expected, the strongest siloxane stretching mode shifted to 1135 cm^{-1} and grew together with the band at 1049 cm^{-1}, while the shoulder band at 1092 cm^{-1}, attributed to the partially hydrolyzed open cubelike species ($T_7(OH)_3$ and $T_8(OH)_4$), disappeared. This indicated condensation between partially hydrolyzed open cubelike species to cubelike or ladderlike condensation products. Actually, the absorption spectrum became similar, but not identical, to the spectra of ladderlike silsesquioxanes,[47] and the corresponding material showed just a single T^3 signal in the ^{29}Si NMR spectra (Figure 10, inset). Because there were no uncondensed silanol groups in the sample heat-treated at 150−200 °C, as inferred from IR and ^{29}Si NMR spectra (Figure 10), the ladder species must be terminated by some arrangement similar to T_8-T_{12} cage molecules. Trifunctional monomer units could act as end groups on the double chain structure, as indicted in Figure 1B. At least up to 200 °C, there was no sign yet of the opening of the double ring cyclic products that terminate ladder species of various lengths. After cooling to room temperature, $MTMSPI^+I^-$ became a solid, amber-like material, which could be reheated without losing its mass, demonstrating the properties of ionic liquids. The material was not electrically conductive at room temperature but started to conduct current at 100 °C ($\sigma = 0.1-0.2$ mS/cm). The absence of electrical conductivity was attributed to the fact that it exhibited two glass transition temperatures at 25 and 65 °C, which lie above room temperature, in contrast to the T_g value (−49.6 °C) of the aged $MTMSPI^+I^-/HCl_{aq}$.

Conclusions

In this study we showed that a new sol−gel precursor, based on a dialkylimidazolium cation terminated with trialkoxysilyl end groups in a quasi solid state consists of positively charged polyhedral cubelike silsesquioxanes. Time-dependent IR ATR and ^{29}Si NMR spectra measurements revealed that, over the course of the first 10 h after addition of acidified water catalyst, the $MTMSPI^+I^-$ precursor underwent simultaneous hydrolysis and condensation reactions. Later, the condensation process prevailed and open cubelike and cubelike species became the dominant products of the condensation reactions. The change of the hydrolyzed $MTMSPI^+I$ sol to a quasi solid state was followed with viscosity measurements which showed that at ambient conditions solidification is achieved in 17 days and that during the condensation the sol remained a Newtonian liquid. This fact suggested that the type of interactions between the species formed in the course of condensation did not change and that no additional cross-linking sites formed during the growth of the condensation species. The final stage of condensation was achieved by heating the sol at 200 °C. The corresponding material exhibited just a single T^3 ^{29}Si NMR signal, implying the presence of trisiloxane linkages, while the absence of silanol groups and the presence of bands at 1135 and 1051 cm^{-1} observed in the IR spectra suggested, in combination with NMR data, that the condensation products consisted of ladderlike silsesquioxanes with terminating cubelike species.

The condensation of sols to a quasi solid state was accompanied by changes in the specific conductivity. It decreased with time of aging and became constant after 15−20 days, achieving a value of about 0.11 mS/cm, which was close to the σ value of the nonhydrolyzed $MTMSPI^+I^-$ ($\sigma = 0.23$ mS/cm). Apparent diffusion coefficients (D_{app}'s) determined for I^- and I_3^- changed in a similar way with time, independently demonstrating the I^-/I_3^- ionic conductivity of the novel electrolyte. Preliminary tests of the DSPEC cell made with this electrolyte, which showed an efficiency of about 3−3.3%, justifies further studies of the synthesized quasi-solid-state electrolyte.

Acknowledgment. This work was supported by the Ministry for Higher Education, Science and Technology and Ministry of Defense of the Republic of Slovenia. V.J. and R.J. thank the former Ministry for the Ph.D. grant. The authors are indebted to Dr. M. Gaberšček and Dr. Lidija Slemenik Perše for their help in performing the conductivity and viscosity measurements.

References and Notes

(1) Tsubomura, H.; Matsumura, M.; Nomura, Y.; Amamiya, T. *Nature* **1976**, *261*, 402.
(2) O'Regan, B.; Graetzel, M. *Nature* **1991**, *353*, 737.
(3) Hagfeldt, A.; Graetzel, M. *Chem. Rev.* **1995**, *95*, 49.
(4) Wang, P.; Zakeeruddin, S. M.; Nazeeruddin, M. K.; Sekiguchi, T.; Graetzel, M.; Moser, E. *Nat. Mater.* **2003**, *2*, 402.
(5) Wang, P.; Zakeeruddin, S. M.; Humphry-Baker, R.; Moser, J. E.; Graetzel, M. *Adv. Mater.* **2003**, *15*, 2101.
(6) O'Regan, B.; Swartz, D. T.; Zakeeeruddin, S. M.; Graetzel, M. *Adv. Mater.* **2000**, *12*, 1263.
(7) Kumura, G. R. A.; Konno, A.; Shiratsuchi, K.; Tsukahara, J.; Tennakone, K. *Chem Mater.* **2002**, *14*, 954.
(8) O'Regan, B.; Lenzmann, F.; Muis, R.; Wienke, J. *Chem. Mater.* **2002**, *14*, 5023.
(9) Taguchi, T.; Zhang, X.; Sutanto, I.; Tokuhiro, K.; Rao, Tn.; Watanabe, H.; Nakamori, T.; Uragami, M.; Fujishima, A. *Chem. Commun.* **2003**, 2480.
(10) Bach, U.; Lupo, D.; Comte, P.; Moser, J. E.; Weissoertel, F.; Salbeck, J.; Spreitzer, H.; Graetzel, M. *Nature* **1998**, *395*, 583.
(11) Krueger, J.; Plass, R.; Graetzel, M.; Matthieu, H. *J. Appl. Phys. Lett.* **2002**, *81*, 367.
(12) Kitamura, T.; Maitani, M.; Matsuda, M.; Wada, Y.; Yanagida, S. *Chem. Lett.* **2001**, 1054.
(13) Nogueira, A. F.; Durrant, J. R.; De Paoli, M.-A. *Adv. Mater.* **2001**, *13*, 826.
(14) Stergiopoulos, T.; Arabatzis, I. M.; Katsaros, G.; Falaras, P. *Nano Lett.* **2002**, *2*, 1259.
(15) Asano, T.; Kubo, T.; Nishikitani, Y. *J. Photochem. Photobiol., A* **2004**, *164*, 111.

(16) Komiya, R.; Han, L.; Yamanaka, R.; Islam, A.; Mitate, T. *J. Photochem. Photobiol., A* **2004**, *164*, 123.
(17) Stathatos, E.; Lianos, P.; Lavrenčič-Štangar, U.; Orel, B. *Adv. Mater.* **2002**, *14*, 354.
(18) Stathatos, E.; Lianos, P.; Šurca Vuk, A.; Orel, B. *Adv. Funct. Mater.* **2004**, *14*, 45.
(19) Stathatos, E.; Lianos, P.; Jovanovski, V.; Orel, B. *J. Photochem. Photobiol., A* **2005**, *169*, 57.
(20) Lavrenčič-Štangar, U.; Orel, B.; Šurca Vuk, A.; Sagon, G.; Colomban, Ph.; Stathatos, E.; Lianos, P. *J. Electrochem. Soc.* **2002**, *149*, E413.
(21) Bonhote, P.; Dias, A. P.; Papageorgiou, N.; Kalyanasundaram, K.; Graetzel, M. *Inorg. Chem.* **1996**, *35*, 1168.
(22) Kawano, R.; Matsui, H.; Matsuyama, C.; Abu Bin Hasan Susan, Md.; Tanabe, N.; Watanabe, M. *J. Photochem. Photobiol., A* **2004**, *164*, 87.
(23) Matsui, H.; Okada, K.; Kawashima, T.; Ezure, T.; Tanabe, N.; Kawano, R.; Watanabe, M. J. *Photochem. Photobiol., A* **2004**, *164*, 129.
(24) Wang, P.; Zakeeruddin, S. M.; Compte, P.; Exnar, I.; Graetzel, M. *J. Am. Chem. Soc.* **2003**, *125*, 1166.
(25) Usui, H.; Matsui, H.; Tanabe, N.; Yanagida, S. *J. Photochem. Photobiol., A* **2004**, *164*, 97.
(26) Kubo, W.; Makimoto, Y.; Wada, Y.; Kitamura, T.; Yanagida, S. *Chem. Lett.* **2002**, 948.
(27) Wang, P.; Zakeeruddin, S. M.; Exnar, I.; Graetzel, M. *Chem. Commun.* **2002**, 2972.
(28) Fuller, J.; Breda, A. C.; Carlin, R. T. *J. Electrochem. Soc.* **1997**, *144*, L67.
(29) Kubo, W.; Kittamura, T.; Nanabusa, K.; Wada, Y.; Yanagida, S. *Chem. Commmun.* **2002**, 247.
(30) Murai, S.; Mikoshiba, S.; Sumio, H.; Hayase, S. *J. Photochem. Photobiol., A* **2002**, *148*, 33.
(31) Kubo, W.; Kambe, S.; Nakade, S.; Kitamura, T.; Hanabusa, K.; Wada, Y.; Yanagida, S. J. *Phys. Chem. B* **2003**, *107*, 4374.
(32) Sakaguchi, S.; Ueli, H.; Kato, T.; Shiratuchi, R.; Takashima, W.; Kaneto, K.; Hayase, S. *J. Photochem. Photobiol., A* **2004**, *164*, 117.
(33) Suzuki, K.; Yamaguchi, M.; Hotta, S.; Tanabe, N.; Yanagida, S. *J. Photochem. Photobiol., A* **2004**, *164*, 81.
(34) Li, W.; Kang, J.; Fang, X.; Lin, Y.; Wang, G.; Xiao, X. *J. Photochem. Photobiol., A* **2004**, *170*, 1.
(35) Kang, J.; Fang, S. *Polym. Bull.* **2002**, *49*, 127.
(36) Voronkov, M. G.; Lavrentyev, V. I. *Top. Curr. Chem.* **1982**, *102*, 199.
(37) Nalwa, H. S. *Handbook of Organic−Inorganic Hybrid Materials and Nanocomposites*; American Scientific Publishers: Stevenson Ranch, CA, 2003; Vol. 1, Chapter 3, p 125.
(38) Sugahara, Y.; Okada, S.; Sato, S.; Kuroda, K.; Kato, C. *J. Non-Cryst. Solids* **1994**, *167*, 21.
(39) Jitianu, A.; Britchi, A.; Deleanu, C.; Badescu, V.; Zaharescu, M. *J. Non-Cryst. Solids* **2003**, *319*, 263.
(40) Brunet, F. *J. Non-Cryst. Solids* **1998**, *231*, 58.
(41) Zhang, Z.; Tanigami, Y.; Terai, R.; Wakabayashi, H. *J. Non-Cryst. Solids* **1995**, *189*, 212.
(42) Zhang, Z.; Wakabayashi, H.; Akai, T. *J. Sol-Gel Sci. Technol.* **1998**, *12*, 153.
(43) Sakka, S.; Tanaka, Y.; Kokubo, T. *J. Non-Cryst. Solids* **1986**, *82*, 24.
(44) Sprung, K. M.; Guenther, F. P. *J. Polym. Sci.* **1958**, *28*, 17.
(45) Brown, J. F. *J. Am. Chem. Soc.* **1965**, *87*, 4317.
(46) Brown, J. F.; Vogt, L. H. *J. Am. Chem. Soc.* **1965**, *87*, 4313.
(47) Brown, J. F. *J. Polym. Sci., A* **1963**, Part C (No. 1), 83.
(48) Brown, J. F.; Vogt, L. H.; Katchman, A.; Eustace, J. W.; Kaiser, K. M.; Krantz, K. W. *J. Am. Chem. Soc.* **1960**, *82*, 6194.
(49) Brown, J. F.; Vogt, L. H.; Prescott, P. I. *J. Am. Chem. Soc.* **1964**, *86*, 1120.
(50) Vogt, L. H.; Brown, J. F. *Inorg. Chem.* **1963**, *2*, 189.
(51) Frye, C. L.; Collins, W. T. *J. Am. Chem. Soc.* **1970**, *92*, 5568.
(52) Bornhauser, P.; Calzaferri, G. *Spectrochim. Acta, Part A* **1990**, *46A*, 1045.
(53) Baertsch, M.; Bornhauser, P.; Buergy, H.; Calzaferri, G. *Spectrochim. Acta, Part A* **1991**, *47A*, 1627.
(54) Baertsch, M.; Bornhauser, P.; Calzaferri, G.; Imhof, R. *Vibr. Spectrosc.* **1995**, *8*, 305.
(55) Baertsch, M.; Bornhauser, P.; Calzaferri, G.; Imhof, R. *J. Phys. Chem.* **1994**, *98*, 2817.
(56) Bornhauser, P.; Calzaferri, G. *J. Phys. Chem.* **1996**, *100*, 2035.
(57) Brinker, C. J.; Scherrer, G. W. *Sol-Gel Science*; Academic Press: Boston, 1990; Chapter 3.
(58) Sassi, Z.; Bureau, J. C.; Bakkali, A. *Vibr. Spectrosc.* **2002**, *28*, 251.
(59) Sassi, Z.; Bureau, J. C.; Bakkali, A. *Vibr. Spectrosc.* **2002**, *28*, 299.
(60) Yoshino, H.; Kamiya, K.; Nasu, H. *J. Non-Cryst. Solids* **1990**, *126*, 68.
(61) Bertie, J. E.; Lan, Z. D. *J. Chem. Phys.* **1996**, *105*, 8502.
(62) Gradadolnik, J. *Acta Chim. Slov.* **2002**, *49*, 631.
(63) Orel, B.; Ješe, R.; Lavrenčič Štangar, U.; Grdadolnik, J.; Puchberger, M. *J. Non-Cryst. Solids* **2005**, *351*, 530.
(64) Orel, B.; Ješe, R.; Vilčnik, A.; Mali, G. *J. Sol-Gel Sci. Technol.*, in press.
(65) Kline, A. A.; Mullims, M. E.; Cornilsen, B. C. *J. Am. Ceram. Soc.* **1991**, *74*, 2559.
(66) Dire, S.; Pagani, E.; Babonneau, F.; Ceccato, R.; Carturan, G. *J. Mater. Chem.* **1997**, *7*, 67.
(67) Deng, Q.; Moore, R. B.; Mauritz, K. A. *Chem. Mater.* **1995**, *7*, 2259.
(68) Robertson, M. A. F.; Mauritz, K. A. *J. Polym. Sci., Polym. Phys.* **1998**, *36*, 595.
(69) Papageorgiou, N.; Athanassov, Y.; Armand, M.; Bonhote, P.; Pettersson, H.; Azam, A.; Graetzel, M. *J. Electrochem. Soc.* **1996**, *143*, 3099.
(70) Stegemann, H.; Rohde, A.; Reiche, A.; Schnittke, A.; Fuellbier, H. *Electrochim. Acta* **1992**, *37*, 379.
(71) Collinson, M. M.; Zambrano, P.; Wang, H.; Taussig, J. *Langmuir* **1999**, *15*, 662.
(72) Niedziolka, J.; Opallo, M. *Electrochem. Commun.* **2003**, *5*, 924.
(73) Opallo, M.; Kukulka-Walkiewicz, J. *Electrochim. Acta* **2001**, *46*, 4235.
(74) Denault, G.; Mirkin, M. V.; Bard, A. J. *J. Electroanal. Chem.* **1991**, *308*, 27.
(75) Loy, D. A.; Baugher, B. M.; Baugher, C. R.; Schneider, D. A.; Rahimian, J. *Chem. Mater.* **2000**, *12*, 3624.
(76) Devreux, F.; Boilot, J. P.; Chaput, F. *Phys. Rev. A* **1990**, *A41*, 6901.
(77) Launer, P. J. *Infrared Analysis of Organosilicon compounds: spectra-structure correlations*; Gelest Inc.: Tullytown, PA, 1998.
(78) Ignatyev, I. S.; Lazarev, A. N.; Tenisheva, T. F.; Shchegolev, B. F. *J. Mol. Struct.* **1991**, *244*, 193.
(79) Koehl, M. *Proc. Estonian Acad. Sci. Chem.* **2000**, *49*, 145.
(80) Bellamy, L. J. *The Infra-red Spectra of Complex Molecules*; John Wiley: London, 1954.
(81) Wright, N.; Hunter, M. J. *J. Am. Chem. Soc.* **1947**, *69*, 803.
(82) Smith, A. C.; Anderson, D. R. *Appl. Spectrosc.* **1984**, *38*, 822.